BAYESIAN POLYNOMIAL REGRESSION OF MAGNETIC-FIELD-DEPENDENT HEAT CAPACITY DATA

AMANDA GIN

Abstract. Alternatively to using a conventional or single point estimate (frequentist) approach to modeling experimental heat capacity data, we utilized a Bayesian modeling framework to get a distribution of possible model parameters (posterior probability). With this method, we investigated a set of experimental heat capacity data from three manganese-based complexes with quantum applications using code written in R Studio to compute the Bayesian quadratic, cubic, fourth-order, fifth-order, and sixth-order polynomial regressions. We made use of the Bayesian statistical approach, incorporating prior knowledge of our parameters (prior probabilities) in the regressions. In general, as the order of the Bayesian polynomial regression fits increased, the "goodness of fit" (inversely proportional to σ) of the model to the experimental data increased. However, the goodness of fit did not increase from a Bayesian fifth to sixth-order polynomial regression. With this information, we hypothesized that experimental heat capacity can be fit with a maximally in the fifth order with respect to temperature.

1. Introduction

Heat capacity or specific heat capacity is a physical property of matter defined as the amount of heat in Joules needed to increase one mole of a material by one temperature degree, C_p ($J/mol \cdot K$). Modeling the heat capacity behavior in molecules is an essential step towards understanding quantum objects at a molecular level. Conventionally, experimental heat capacity data is fit using linear combinations of well-established equations with physical origins (see the appendix).

In this work, we take an alternative mathematical approach to modeling a set of experimental low-temperature (1 to 50 K = -272 to -223 C = -458 to -370 F) heat capacity data of three manganese-based complexes **1-3** using Bayesian polynomial regressions.

1.1. Frequentist Approach: Ordinary Least Squares Polynomial Regression (OLS).

In general, the aim of regression analysis is to model the expected value of a response variable in terms of a linear combination of predictor variables, (x_i) with coefficients, β_i [5]. β_i are known as the model parameters. α is a constant intercept term. The full formula includes an term to account for the unexplained random variance between the data and the regression model, expressed as ϵ [1]. This method assumes the predictor variables are random samples and predicts the response variable as a point estimate. We call this a frequentist approach, which is different from a Bayesian approach, which we will discuss later [1]. The general polynomial regression model is shown below in Equation 1.

$$f(x) = \alpha + \sum_{i=1}^{n} x_i \beta_i + \epsilon \tag{1}$$

OLS is the most basic and most popular method in polynomial regression analysis. The method finds the coefficients β_i that best explain the data. It does this by focusing on

Date: February 26, 2024.

minimizing the residual sum of squares (RSS, Equation 2) between the observed data and the fitted value provided by a polynomial regression model by optimizing the β_i's [1].

$$\text{RSS}(\beta) = \sum_{i=1}^{n}(y_i - f(x_i))^2 = \sum_{i=1}^{n}(y_i - \beta_i x_i)^2 \tag{2}$$

The OLS polynomial regression model that has the lowest RSS value (closest to zero) is determined to be model of best fit for the set of experimental data. The frequentist approach using OLS is relatively simple and often times quite effective depending on the dataset. However, this method is also extremely limited in that is can only output a point estimate for the parameters and does not allow incorperation of prior knowledge.

1.2. **Bayesian Framework.** The Bayesian approach to polynomial regression operates a few core principles, namely Bayes' Theorem (Theorem 1.1)

Theorem 1.1. Posterior Probability $= \frac{\text{Likelihood} * \text{Prior Probability}}{\text{Normalization}}$

The posterior probability distribution is defined as "the distribution of an unknown quantity, treated as a random variable, conditional on the evidence obtained." This is equal to the likelihood of the data with respect to the model multiplied by the prior probability of the parameters and divided by a normalization constant.

Bayes' theorem allows us to include initial guesses (by setting prior probabilities) for what the model parameters should be, unlike in the frequentist approach, which assumes that the parameters come directly from the data [1]. Using the Bayesian method outputs a distribution of possible model parameters (posterior probability) based on the data and the priors.

1.3. **Bayesian Approach: Bayesian Polynomial Regression.** Bayesian polynomial regression is a type of polynomial regression that uses principles of Bayesian statistics to estimate the likelihood of a set of parameters from experimental data. This method makes it possible to recover a range of plausible solutions.

We formulate the approach using probability distributions rather than point estimates (frequentist approach). The goal of Bayesian polynomial regression is slightly different from classical polynomial regression: Bayesian polynomial regression aims to not find the single "best" value of the model parameters, but rather to determine to posterior distribution for the model parameters [1]. The Bayesian view also assumes that the response variable, y, is not estimated by a single value, but assumes it is drawn from a probability (normal/Gaussian) distribution (Equation 3) [1]:

$$y \backsim N\left(\beta\mathbf{X}, \sigma^2\right) \tag{3}$$

Observe that the response variable is now a normal distribution with mean, $\beta\mathbf{X}$ and variance σ^2. $\beta\mathbf{X}$ is the general linear equation in $\mathbf{X}$ which is the matrix of x_i's .

Another advantage to this method is that it can take into account prior knowledge about the parameters which are input by the modeler. With information about the priors, the method sets an initial model as "null hypothesis" and tests against it with the experimental data. Due to its probabilistic character, this method can produce more accurate estimates for regression parameters which can help to make stronger conclusions than classical regression techniques.

In summary, Bayesian polynomial regression provides two critical advantages [2]:

(1) **Priors:** We can include any prior knowledge we have by placing prior probability distributions on the parameters. For example, if we think that σ is small, we could choose a probability distribution of $N(0, 1)$.
(2) **Quantifying uncertainty:** We get a posterior distribution for our β_i's rather than a point estimate. This is advantageous for small data sets with high uncertainties in β_i's with wide posterior distributions.

2. Problem formulation

In the present literature, there several works measuring the low-temperature specific heat capacity of perovskites [12] and single-molecule magnets [11, 13]. These works primarily focus on the obvious detection of interesting crystallographic and/or magnetic phase transitions. Several authors only briefly discuss their modeling method of their experimental heat capacity data, if at all. Moreover, there are even fewer works [13] that fit experimental heat capacity at variable fields. The authors that do elaborate on how they modeled their experimental heat capacity data utilize linear combinations of well-established physical models – such as those discussed in the appendix. In most cases, extensive prior expertise knowledge of the physical system or a brute force approach is used to model experimental heat capacity data. The aforementioned has been the acceptable approach to modeling heat capacity for decades.

We aim to explore a new approach to this modeling problem using a mathematical basis. With Bayesian polynomial regression, we gather a plausible set of solutions and can potentially discriminate heat capacity's order with respect to temperature.

3. Our method

The heat capacity data for **1-3** were pooled by field (0, 1, 2 T). We used Bayesian quadratic, cubic, fourth-order, fifth-order, and sixth-order polynomial regression models on the experimental heat capacity data. We omitted fitting the experimental heat capacity data using a Bayesian linear polynomial regression, since the data are clearly non-linear and contains some degree of curvature (Figure 1).

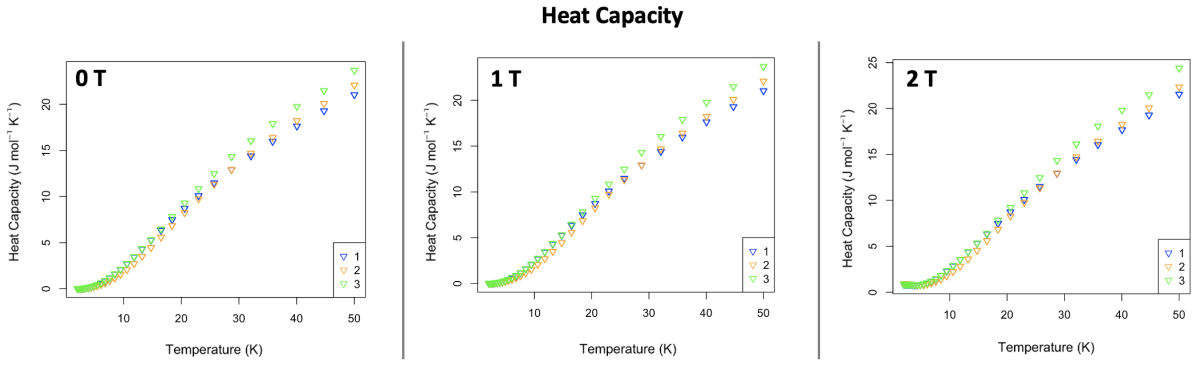

Figure 1. Experimental heat capacity data of **1-3** at 0, 1, and 2 T.

4. Experimental

First, as a precaution, the temperature (predictor) data were standardized to account for precision numerical errors with computation of very small or large values. Normalized heat capacity data of **1-3** is shown below in Figure 2.

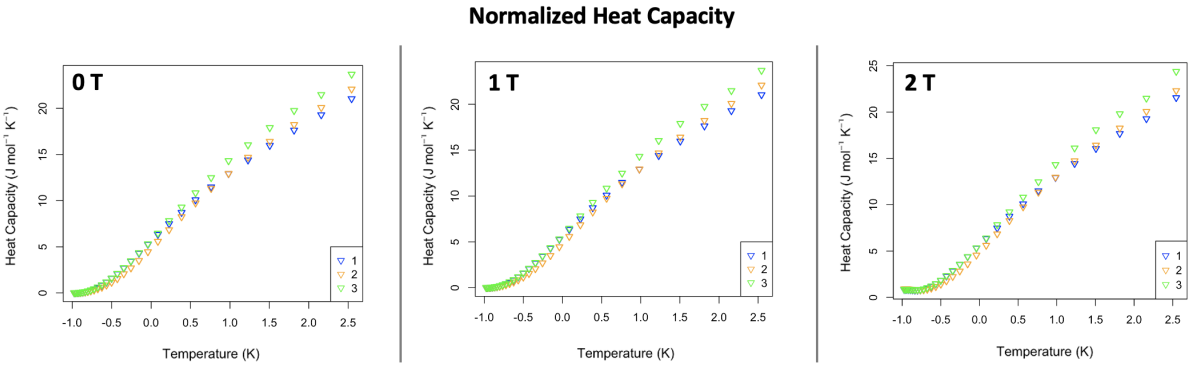

Figure 2. Normalized experimental heat capacity data of **1-3** at 0, 1, and 2 T.

The Bayesian quadratic, cubic, fourth-order, fifth-order, and sixth-order models shown below in Tables 1-4 were tested using code adapted from Sergio Marrero, written in R Studio [3]. Scripts and raw data can be found at `https://github.com/goa225/MnHeatCapacity`.

Table 1: Bayesian quadratic regression model.

Bayesian Quadratic Regression Models	
Quadratic Model	Definition
$h_i \backsim N(\mu_i, \sigma)$	Likelihood
$\mu_i = \alpha + \beta_1 x_i + \beta_2 x_i^2$	Quadratic Model
$\alpha \backsim N(0, 10)$	Prior for α
$\beta_1 \backsim N(0, 10)$	Prior for β_1
$\beta_2 \backsim N(0, 10)$	Prior for β_2
$\sigma \backsim U(0, 1)$	Prior for σ

Table 2: Bayesian cubic regression model.

Bayesian Cubic Regression Models	
Cubic Model	Definition
$h_i \backsim N(\mu_i, \sigma)$	Likelihood
$\mu_i = \alpha + \beta_1 x_i + \beta_2 x_i^2 + \beta_3 x_i^3$	Cubic Model
$\alpha \backsim N(0, 10)$	Prior for α
$\beta_1 \backsim N(0, 10)$	Prior for β_1
$\beta_2 \backsim N(0, 10)$	Prior for β_2
$\beta_3 \backsim N(0, 10)$	Prior for β_3
$\sigma \backsim U(0, 1)$	Prior for σ

Table 3: Bayesian fourth-order regression model.

Bayesian Fourth-Order Regression Models	
Fourth-Order Model	Definition
$h_i \backsim N(\mu_i, \sigma)$	Likelihood
$\mu_i = \alpha + \beta_1 x_i + \beta_2 x_i^2 + \beta_3 x_i^3 + \beta_4 x_i^4$	Fifth-Order Model
$\alpha \backsim N(0, 10)$	Prior for α
$\beta_1 \backsim N(0, 10)$	Prior for β_1
$\beta_2 \backsim N(0, 10)$	Prior for β_2
$\beta_3 \backsim N(0, 10)$	Prior for β_3
$\beta_4 \backsim N(0, 10)$	Prior for β_4
$\sigma \backsim U(0, 1)$	Prior for σ

Table 4: Bayesian fifth-order regression model.

Bayesian Fifth-Order Regression Models	
Fifth-Order Model	Definition
$h_i \backsim N(\mu_i, \sigma)$	Likelihood
$\mu_i = \alpha + \beta_1 x_i + \beta_2 x_i^2 + \beta_3 x_i^3 + \beta_4 x_i^4 + \beta_5 x_i^5$	Fifth-Order Model
$\alpha \backsim N(0, 10)$	Prior for α
$\beta_1 \backsim N(0, 10)$	Prior for β_1
$\beta_2 \backsim N(0, 10)$	Prior for β_2
$\beta_3 \backsim N(0, 10)$	Prior for β_3
$\beta_4 \backsim N(0, 10)$	Prior for β_4
$\beta_5 \backsim N(0, 10)$	Prior for β_5
$\sigma \backsim U(0, 1)$	Prior for σ

Table 5: Bayesian sixth-order regression model.

Bayesian Sixth-Order Regression Models	
Sixth-Order Model	Definition
$h_i \backsim N(\mu_i, \sigma)$	Likelihood
$\mu_i = \alpha + \beta_1 x_i + \beta_2 x_i^2 + \beta_3 x_i^3 + \beta_4 x_i^4 + \beta_5 x_i^5 + \beta_6 x_i^6$	Sixth-Order Model
$\alpha \backsim N(0, 10)$	Prior for α
$\beta_1 \backsim N(0, 10)$	Prior for β_1
$\beta_2 \backsim N(0, 10)$	Prior for β_2
$\beta_3 \backsim N(0, 10)$	Prior for β_3
$\beta_4 \backsim N(0, 10)$	Prior for β_4
$\beta_5 \backsim N(0, 10)$	Prior for β_5
$\beta_6 \backsim N(0, 10)$	Prior for β_6
$\sigma \backsim U(0, 1)$	Prior for σ

Since we have no initial knowledge of what the parameter distributions should look like in this scenario, for simplicity, we assumed the that the parameter prior probabilities were normally distributed around zero with a variance of 10. We tested prior probabilities with different means and variances than that mentioned before, though encountered computational errors stating the initial guesses were too far when trying to fit the experimental data in R Studio. For example, one such prior that did not work was $\beta_1 \backsim N(10, 2)$. For computation using the Bayesian approach, the initial parameter priors must be in "reasonable range" to the final calculated values or the algorithm will diverge. We also made the assumption that σ was uniformly distributed for similar reasons.

5. Results

The Bayesian quadratic, cubic, fourth-order, fifth-order, and sixth-order polynomial regression fits for the experimental heat capacity data of **1-5** are shown below in Figure 3. The 89% prediction interval for the data are indicated by the shaded regions. The region in red is the uncertainty (89%) related with the Bayesian polynomial model given the data $(\mu|x)$. The region in grey represents the area within which the model expects to find 89% of the actual heat capacities for each parameter (between values under 5.5% to 94.5% in Tables 6-10) [4].

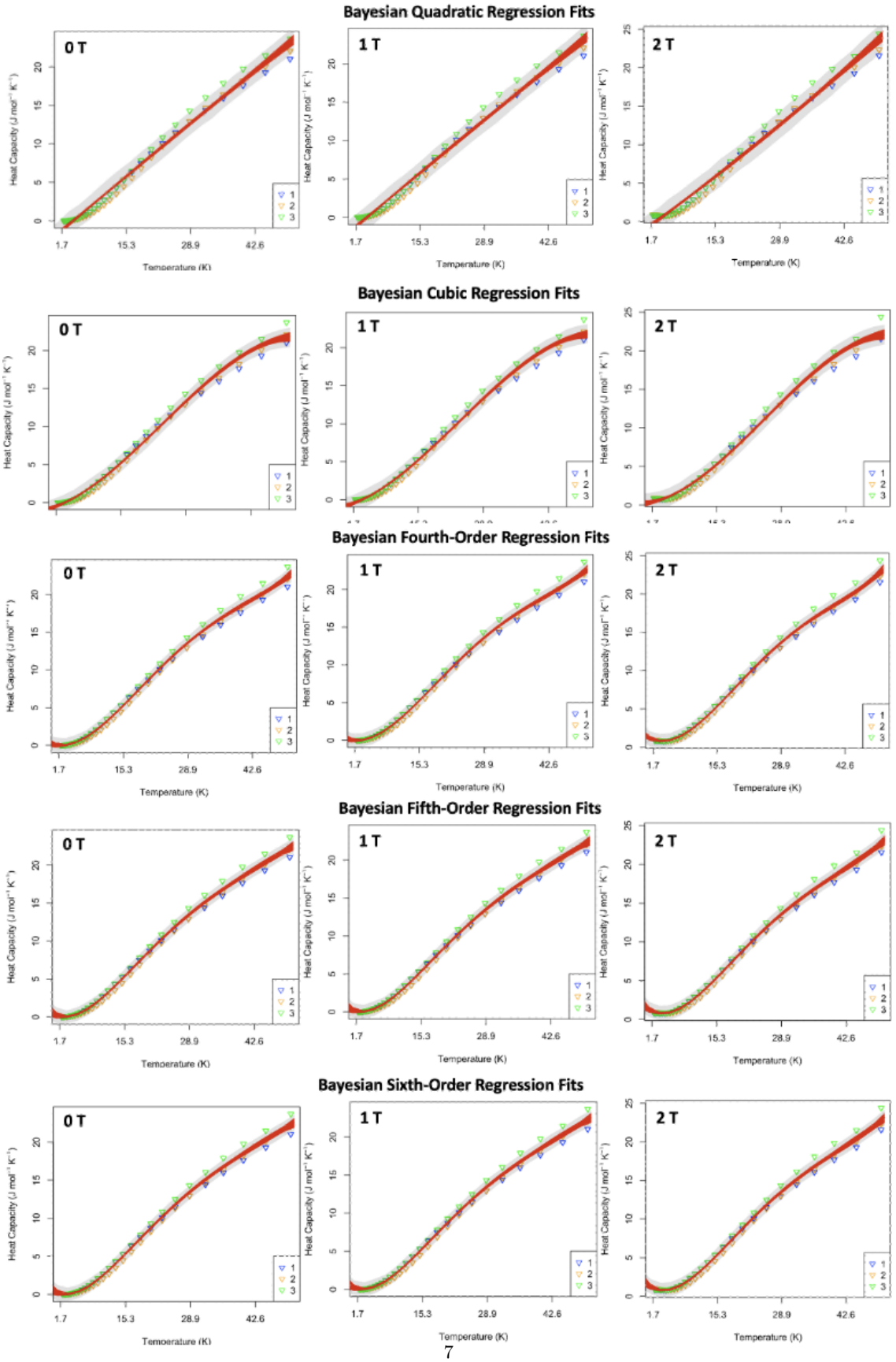

FIGURE 3. Bayesian quadratic, cubic, fourth-order, and fifth-order regressions for experimental heat capacity data of **1-3** at 0, 1, and 2 T.

The corresponding outputted Bayesian regression fit parameters are summarized below in Tables 6-10.

Table 6: Parameters from Bayesian quadratic regression of experimental heat capacity data of **1-3**.

Bayesian Quadratic Regression Models												
	0 T				1 T				2 T			
Parameter	Mean	SD	5.5%	94.5%	Mean	SD	5.5%	94.5%	Mean	SD	5.5%	94.5%
α	5.79	0.12	5.60	5.98	5.84	0.13	5.63	6.05	5.88	0.13	5.67	6.09
β_1	6.95	0.12	6.75	7.15	6.78	0.13	6.55	6.87	6.50	0.14	6.28	6.73
β_2	-0.05	0.09	-0.19	0.09	0.9	0.10	-0.09	0.19	0.19	0.10	0.04	0.35
σ	0.78	0.06	0.68	0.87	0.84	0.06	0.073	0.92	0.86	0.06	0.076	0.96

Table 7: Parameters from Bayesian cubic regression of experimental heat capacity data of **1-3**.

Bayesian Cubic Regression Models												
	0 T				1 T				2 T			
Parameter	Mean	SD	5.5%	94.5%	Mean	SD	5.5%	94.5%	Mean	SD	5.5%	94.5%
α	5.24	0.10	5.07	5.40	5.25	0.10	5.07	5.22	5.26	0.11	5.08	5.44
β_1	7.24	0.11	7.37	7.72	7.30	0.11	7.12	7.51	7.17	0.12	6.98	7.23
β_2	1.19	0.15	0.95	1.42	1.32	0.15	1.08	1.52	1.58	0.16	1.33	1.84
β_3	-0.63	0.07	-0.74	-0.52	-0.65	0.07	-0.78	0.53	-0.71	0.07	-0.83	-0.60
σ	0.55	0.04	0.49	0.62	0.57	0.04	0.50	0.64	0.60	0.04	0.53	0.67

Table 8: Parameters from Bayesian fourth-order regression of experimental heat capacity data of **1-3**.

Bayesian Fourth-Order Regression Models												
	0 T				1 T				2 T			
Parameter	Mean	SD	5.5%	94.5%	Mean	SD	5.5%	94.5%	Mean	SD	5.5%	94.5%
α	5.28	0.09	5.14	5.42	5.29	0.09	5.15	5.43	5.31	0.09	5.17	5.45
β_1	8.57	0.18	8.28	8.77	8.57	0.18	8.28	8.75	8.43	0.19	8.13	8.72
β_2	1.13	0.12	0.93	1.32	1.32	0.12	1.09	1.42	1.51	0.12	1.32	1.71
β_3	-1.75	0.18	-2.04	-1.46	-1.87	0.18	-2.13	-1.56	-2.08	0.18	-2.37	-1.78
β_4	0.40	0.06	0.30	0.50	0.44	0.03	0.35	0.52	0.49	0.06	0.39	0.59
σ	0.46	0.03	0.40	0.51	0.46	0.03	0.40	0.51	0.46	0.03	0.41	0.52

Table 9: Parameters from Bayesian fifth-order regression of experimental heat capacity data of **1-3**.

Bayesian Fifth-Order Regression Models												
	0 T				1 T				2 T			
Parameter	Mean	SD	5.5%	94.5%	Mean	SD	5.5%	94.5%	Mean	SD	5.5%	94.5%

α	5.36	0.10	5.20	5.52	5.36	0.10	5.20	5.52	5.37	0.10	5.20	5.53
β_1	8.69	0.20	8.37	9.00	8.65	0.20	8.35	8.93	8.51	0.20	8.19	8.83
β_2	0.69	0.32	0.18	1.21	0.95	0.32	0.51	1.72	1.21	0.33	0.68	1.73
β_3	-1.87	0.20	-2.19	-1.56	-1.93	0.20	-2.35	-1.73	-2.17	0.20	-2.49	-1.84
β_4	0.76	0.26	0.35	1.17	0.75	0.26	0.33	1.17	0.74	0.26	0.32	1.16
β_5	-0.10	0.07	-0.21	0.01	-0.08	0.07	-0.20	0.03	-0.07	0.07	-0.19	0.04
σ	0.45	0.03	0.40	0.50	0.45	0.03	0.40	0.50	0.46	0.03	0.41	0.52

Table 10: Parameters from Bayesian sixth-order regression of experimental heat capacity data of **1-3**.

Bayesian Sixth-Order Regression Models												
	0 T				1 T				2 T			
Parameter	Mean	SD	5.5%	94.5%	Mean	SD	5.5%	94.5%	Mean	SD	5.5%	94.5%
α	5.36	0.11	5.20	5.53	5.36	0.11	5.20	5.54	5.37	0.11	5.20	5.56
β_1	8.69	0.25	8.37	9.00	8.65	0.25	8.35	8.94	8.51	0.26	8.19	8.86
β_2	0.69	0.47	0.18	1.21	0.95	0.47	0.51	1.72	1.21	0.47	0.68	1.73
β_3	-1.87	0.49	-2.19	-1.56	-1.93	0.49	-2.35	-1.73	-2.17	0.49	-2.49	-1.84
β_4	0.76	0.36	0.35	1.17	0.75	0.36	0.33	1.17	0.74	0.37	0.32	1.16
β_5	-0.10	0.36	-0.21	0.01	-0.08	0.36	-0.20	0.03	-0.07	0.36	-0.19	0.04
β_6	0.00	0.08	-0.13	0.13	0.00	0.08	-0.13	0.13	0.03	0.08	-0.10	0.17
σ	0.45	0.03	0.40	0.50	0.45	0.03	0.40	0.50	0.46	0.03	0.41	0.52

6. Discussion and future work

The experimental heat capacity data were collected on a log scale in the indicated temperature range. This means that the majority of the data points are collected at lower temperatures. In general, there were also smaller deviations observed in the heat capacity data set at lower temperatures. In combination of the two things mentioned prior, the 89% prediction intervals *in the range of the data collected* are narrower at lower temperatures and wider and higher temperatures across all Bayesian polynomial regression models (see Figure 4 for an example). The 89% prediction interval *outside the temperature region from which the data were collected* is large due to uncertainty in the estimation from no data points at these temperatures (across all models).

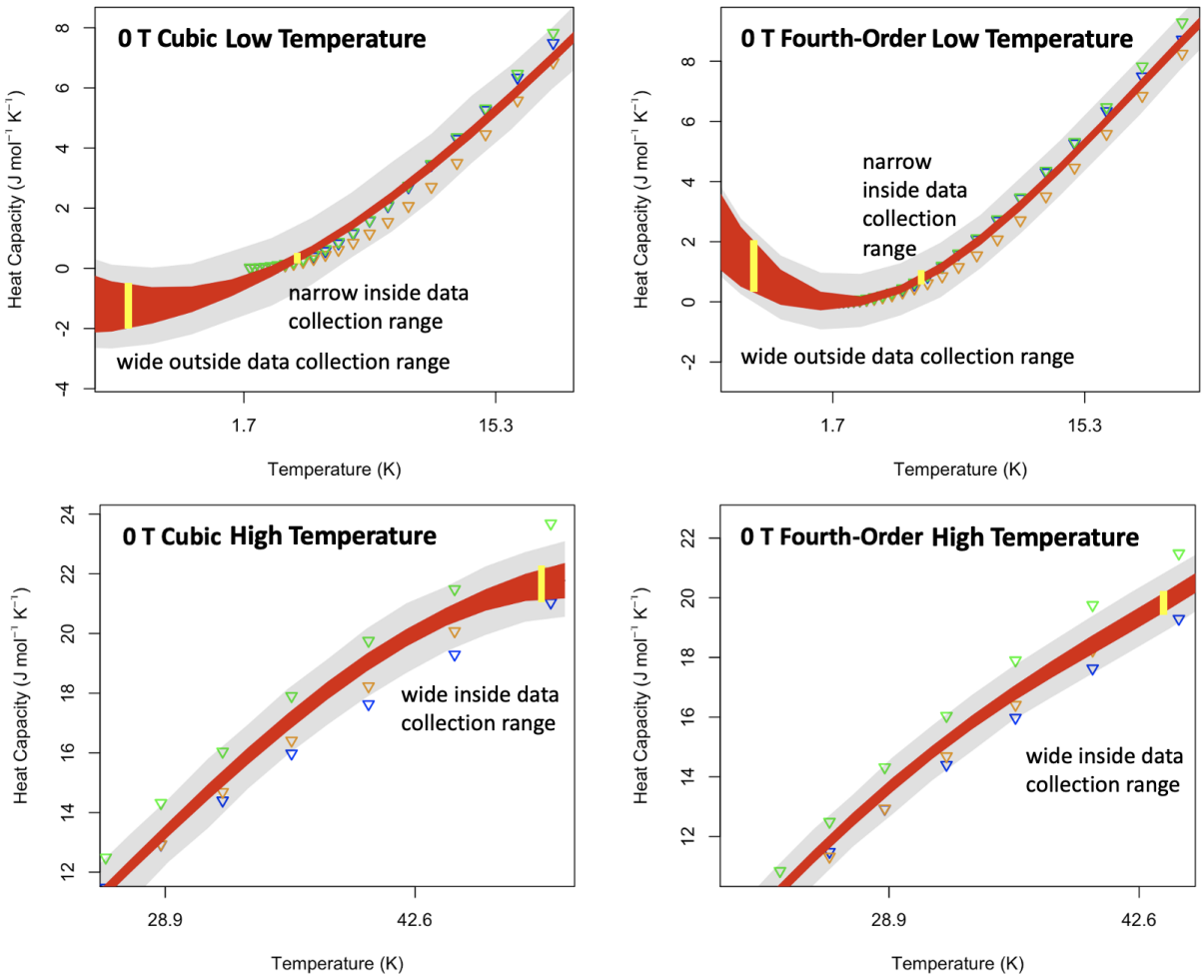

FIGURE 4. Low and high temperature regions of Bayesian quadratic and cubic regressions for experimental heat capacity data of **1-3** at 0 T

.

Not surprisingly, the heat capacity data is least well modeled by the Bayesian quadratic model (Table 6). This model has the highest calculated σ values of 0.78, 0.84, and 0.86 at 0, 1, 2 T, respectively. Interestingly, β_2 is nearly zero, making the Bayesian quadratic model nearly linear. This can be explained by the curvature of the data, whereby it is more statistically favorable to place half of the data above the model and the other half below, than to fit only some data points very well with a quadratic and leave the remaining data with large deviations.

We see improvement in the fitting as we increase the order of the Bayesian polynomial used (see the decreasing σ values. Visually we can especially observe this decreasing deviation when looking at the experimental data in comparison to the Bayesian polynomial regression model at the extremes of the temperature range in which we collected (see Figure 4 for an example). The modeling of the experimental data at the extremes of the temperature range greatly improves from the Bayesian linear to quadratic to cubic model.

Interestingly, the goodness of fit does not appear to increase from a Bayesian fifth-order polynomial regression (Table 9) to a Bayesian sixth-order polynomial regression (Table 10). Indeed, both the Bayesian fifth-order and sixth-order polynomial regression have σ values of 0.55, 0.45, and 0.46 at 0, 1, 2 T, respectively. This indicates that the experimental heat capacity data is likely best fit by a fifth-order polynomial. This is confirmed by the near-zero β_6 coefficient of the Bayesian sixth-order polynomial regression. We hypothesize that heat capacity of these complexes is maximally fifth-order in terms of temperature.

7. Future directions

To confirm the hypothesis stated above: that the heat capacity of these complexes is maximally fifth-order in terms of temperature, we should test Bayesian seventh-order eighth-order,..., n-th order polynomial regressions in order to see if β_7,...,β_n's are all near-zero. This will provide confirmation that the experimental heat capacity is indeed maximally fifth-order with resepct to temperature.

8. Conclusion

Due to the complexity and expertise required to model experimental heat capacity data by conventional means, we explored modeling the data using Bayesian polynomial regression. Unlike in classical regression analysis where we can only find a point estimate, with the Bayesian approach, we get individual distributions for each predictor variable. This allows us to make more powerful and stronger conclusions about the data.

When modeling the experimental heat capacity of set of manganese complexes, we observed that the Bayesian fifth-order polynomial regression was the best fit, with σ values of 0.55, 0.45, and 0.46 at 0, 1, 2 T, respectively. The goodness of fit did not increase in the Bayesian sixth-order polynomial regression model. We hypothesize that heat capacity of these complexes is maximally fourth-order in terms of temperature.

9. Acknowledgements

This research was performed with the support of Colorado State University (CSU), in part by the National Institutes of Health (R21- EB027293) and the Department of Energy (DE-SC0021259). Nuclear magnetic resonance experiments and standard molecular characterization were performed at the CSU Analytical Resources Core (Research Resource ID: SCR_021758), which is supported by an NIH-SIG award (1S10OD021814-01) and the CSU-CORES Program.

10. Appendix

10.1. **Manganese-Based Molecular Complexes.** The three manganese-based complexes whose experimental heat capacities make up the dataset used of this work contain cryptand-derivative ligands: [MnL1]$(PF_6)_2$ (**1**, L1 = 1,4,7,10,13,16,21,24-Octaazabicyclo[8.8.8]hexacosa-4,6,13,15,21,23-hexaene), [MnL2]$(PF_6)_2$ (**2**, L2 = 1,4,7,10,13,16,21,24-Octaazabicyclo[8.8.8]-hexacosane), and [MnL3]$(PF_6)_2$ (**3**, L3 = 17,20,25,28-Tetraoxa-1,14,31,32-tetraazatetracyclo-[12.8.8.$1^{1,3}$.$1^{8,12}$]doctriaconta-3,5,7(32),8,10,12(31)-hexaene) (Figure 5). Synthesis of the studied complexes were carried out according to the literature [6].

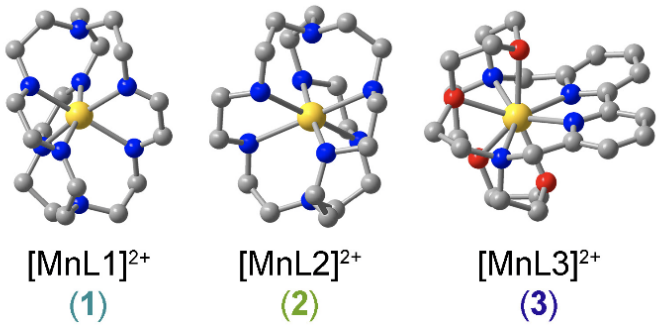

FIGURE 5. Molecular structures of $[MnL1]^{2+}$, $[MnL2]^{2+}$, and $[MnL3]^{2+}$ as determined for **1, 2,** and **3**. Yellow, red, blue, and gray spheres represent Mn, O, N, and C atoms, respectively. Hydrogens, solvent, and PF_6^- counterions have been omitted for clarity.

10.2. **Experimental Heat Capacity Measurements.** We will briefly discuss how the specific heat can be measured. There are several methods for the practical determination of the specific heat capacity of solids. In principle, the simplest way to evaluate the specific heat is to decouple the sample from the surroundings, and apply a known amount of heat to the sample [8]. The temperature of the sample is monitored and variations allow evaluation of C_p. Even in vacuo, this measurement is severely affected by the non-perfect adiabatic condition (ie. the wires of the thermometer and heater, in addition to the sample holder, may be responsible for a thermal leak). Bachmann et al. (1972) developed another method, known as the relaxation method, to account for the linkage between the sample and the thermal bath. This method presents several advantages: adiabaticity is not required and the sample can have poor thermal conductivity.

Heat capacity measurements were performed on microcrystalline samples (approx. 2-4 mg) of **1-3** mounted in Apiezn N Grease using a Physical Properties Measurement System DynaCool (Quantum Design) equipped with a single two-stage Pulse Tube cooler. Data were collected with an applied field of of 0, 1, 2 T in the 50-2 K temperature range with a 1% temperature rise. The data were corrected for the heat capacity contribution from the grease.

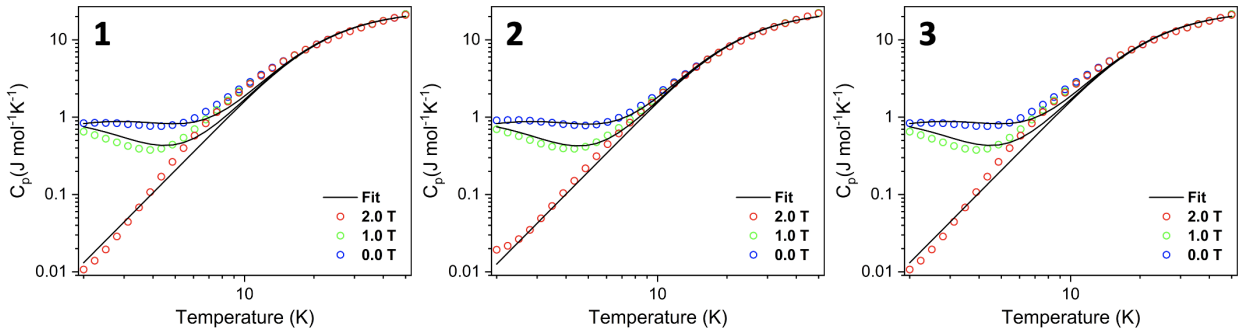

FIGURE 6. Field and temperature dependence of the heat capacities of **1-3** measured from 2 to 50 K plotted on log-log scales. Solid lines are conventional simulations of the heat capacity, see below text for details.

10.3. **Conventional Physical Models of Heat Capacity.** In general, heat capacity can be divided into three contributions (Equation 4): a lattice vibration (C_{lat}), a magnetic Schottky anomaly from spin energy levels (C_{spin}), and a hyperfine interaction that appears at very low temperatures (C_{hf}) [10].

$$C_p = C_{lat} + C_{spin} + C_{hf} \tag{4}$$

The majority of heat capacity behavior at higher temperatures (general curvature) is typically defined by the lattice contribution, C_{lat}. In a perfect crystal there are $3N$ independent modes of lattice vibration, with N the number of ions in a unit cell. Typically one idealizes to three acoustic branches and $(3N-3)$ optical branches [10]. The acoustic branches give rise to the Debye contribution (Equation 5), C_D. Whereas the optical branches give the Einstein contribution (Equation 6), C_E. The derivations of these arise from physical phenomena which are well-described elsewhere (`https://en.wikipedia.org/wiki/Debye_model`). Both Debye and Einstein models often correspond closely to experimental data, though importantly have distinct scales. C_{lat} is often approximated using one of these models or some combination thereof. In general, the Debye model better succeeds in modeling the heat capacity at low temperatures (in materials without a large hyperfine interaction).

$$\frac{C_D}{R} = 9\left(\frac{T}{\theta_D}\right)\int_0^{\theta_D/T}\frac{x^4 e^x}{(e^x-1)^2}dx \tag{5}$$

where C_D is the Debye heat capacity contribution ($\mathrm{J/mol \cdot K}$), R is the ideal gas constant (), T is measurement temperature (K), θ_D is the Debye temperature (K).

$$\frac{C_E}{R} = 3\left(\frac{T_E}{T}\right)^2\frac{\exp\left(\frac{\theta_E}{T}\right)}{\left[\exp\left(\frac{\theta_E}{T}\right)-1\right]^2} \tag{6}$$

where C_E is the Einstein heat capacity contribution ($\mathrm{J/mol \cdot K}$) and θ_E is the Einstein temperature (K).

For $T << \theta_D$ (typically $T \leq \theta_D/50$), the Debye contribution can be well approximated by the simpler model (Equation 7) [10]:

$$\frac{C_D}{R} = 234\left(\frac{T}{\theta_D}\right)^{\alpha} \tag{7}$$

where α Debye exponent, commonly $\alpha = 3$.

The magnetic Schottky anomaly (Equation 8) derived from spin energy levels, C_{spin}, attributes the next largest contribution to the heat capacity behavior (at low temperatures) [9, 10]. This contribution is especially prevalent in variable-field heat capacity studies of molecular materials, which is the focus of this work. The Schottky contribution can be expressed as:

$$\frac{C_S}{R} = \beta^2 \frac{\sum_i E_i^2 \exp\left(-\beta E_i\right) \sum_i \exp\left(-\beta E_i\right) - \left[\sum_i E_i \exp\left(-\beta E_i\right)\right]^2}{\left[\sum_i \exp\left(-\beta E_i\right)\right]^2} \tag{8}$$

where C_S is the Schottky heat capacity contribution ($\mathrm{J/mol \cdot K}$),E_i is the energy of a specific magnetic level (J) assuming population following a canonical Boltzmann distribution, and $\beta = (Tk_B)^{-}1$ with k_B being the Boltzmann constant.

Lastly, the hyperfine interaction which is commonly found in materials that contain unpaired electrons. [11]

$$\frac{C_{hf}}{R} \approx \frac{n}{3} I\left(I+1\right) \left(\frac{h\upsilon_n}{k_B}\right)^2 \frac{1}{T^2} \tag{9}$$

where C_{hf} is the hyperfine heat capacity contribution ($\mathrm{J/mol \cdot K}$). See [11] for an detailed explanation of the hyperfine variables.

10.4. **Application of Conventional Heat Capacity Models to 1-3.** Heat capacities of **1-3** were modeled in the literature [6] using a simple linear combination of Debye (Equation 5) and Schottky (Equation 8) contributions (Figure 6, Equation 10). These heat capacity data were collected at sufficiently low temperatures, thus the Debye model was chosen in preference over the similar Einstein model. The Debye contributions were fit in Python with scipy.optimize.curve_fit (scripts and raw data can be also found at `https://github.com/goa225/MnHeatCapacity`). The Schottky (spin) contribution was modelled in PHI [9]. In these data, a small hyperfine interaction was observed at low temperatures (< 5 K), consistent with other solid-state measurements of **1-3**, and were small enough to be entirely omitted in the model.

$$\frac{C_D + C_S}{R} = 9\left(\frac{T}{\theta_D}\right) \int_0^{\theta_D/T} \frac{x^4 e^x}{(e^x - 1)^2} dx + \beta^2 \frac{\sum_i E_i^2 \exp(-\beta E_i) \sum_i \exp(-\beta E_i) - \left[\sum_i E_i \exp(-\beta E_i)\right]^2}{\left[\sum_i \exp(-\beta E_i)\right]^2} \tag{10}$$

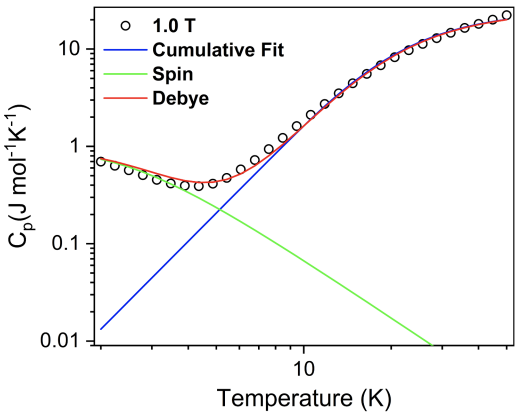

FIGURE 7. Depiction of the two competing contributions (Debye and Schottky) to the heat capacity data for **2** under and applied magnetic field of 1 T.

REFERENCES

[1] Koehrsen, W. *Introduction to Bayesian Linear Regression.* Towards Data Science. (2018); https://towardsdatascience.com/introduction-to-bayesian-linear-regression-e66e60791ea7.

[2] Wiecki, T. *THE INFERENCE BUTTON: BAYESIAN GLMS MADE EASY WITH PYMC.* (2013); https://twiecki.io/blog/2013/08/12/bayesian-glms-1/.

[3] Marrero, S. *Polynomial Regression.* RPubs (2018); https://rpubs.com/SergioMarrero/352161.

[4] Marrero, S. *A bayesian Linear Regression; Reference Book: Statistical Rethinking - Richard McElreath. Chapter 4.* RPubs (2018); https://rpubs.com/SergioMarrero/351562.

[5] Dash, S. *Bayesian Approach to Regression Analysis with Python.* Analytics Vidhya (2022); https://www.analyticsvidhya.com/blog/2022/04/bayesian-approach-to-regression-analysis-with-python/.

[6] Campanella, A; Gin, A; Sung, S; Jackson, C; Martinez, M; Ozarowshi, A; Bhowmick, I; Zadrozny, J. *Amplyfying the Temperature Sensitivity of Zero-Field Splitting in Mn(II) Through Ligand Tuning* ChemRxiv. 2023; doi:10.26434/chemrxiv-2023-hk4dq.

[7] Marin, E; Delgado-Vasallo, O; Valiente, H. *A temperature relaxation method for the measurement of the specific heat of solids at room temperature in student laboratories* American Journal of Physics. 2003; doi:10.1119/1.1586261.

[8] Gatteschi, D; Sessoli, R; Villain, J. *Molecular Nanomagnets* Oxford University Press. 2006; doi:10.1093/acprof:oso/9780198567530.001.0001.

[9] Chilton, N; Anderson, R; Turner, L; Sonicini, A; Murry, K. *PHI: A powerful new program for the analysis of anisotropic monomeric and exchange-coupled polynuclear d- and f-block complexes* Journal of Computational Chemistry. 34 (2013) : 1164–1175; doi:10.1002/jcc.23234.

[10] Evangelisti, M; Luis, F; de Jongh, L; Affronte, M. *Magnetothermal properties of molecule-based materials* Journal of Materials Chemistry. 16 (2006) : 2534–2549; doi:10.1039/B603738K.

[11] Miyazaki, Y; Bhattacharjee, A; Nakano, M; Saito, K; Aubin, S; Eppley, H; Christou, G; Henderickson, D; Sorai, M. *Magnetic-Field-Dependent Heat Capacity of the Single-Molecule Magnet* $[Mn_{12}O_{12}(O_2CEt)_{16}(H_2O)_3]^2$. Inorganic Chemistry. 40 (2001) : 6632–6636; doi:10.1021/ic010567w.

[12] Klemme, S; Hermes, W; Eul, M; Wijbrans, C; Rohrbach, A; Pottgen, R. *New thermodynamic data for* $CoTiO_3$*,* $NiTiO_3$*, and* $CoCO_3$ *based on low-temperature calorimetric measurements.* Chemistry Central Journal. 54 (2011); doi:10.1186/1752-153X-5-54.

[13] Rubin-Osanz, M; Lambert, F; Shao, F; Riviere, E; Guillot, R; Suaud, N; Guihery, N; Zueco, D; Barra, A; Mallah, T; Luis, F. *Chemical tuning of spin clock transitions in molecular monomets based on nuclear spin-free Ni(II).* Chemical Science. 12 (2021) : 5123; doi:10.1039/d0sc05856d.